Journal of Nuclear Materials 377 (2008) 396–400

Contents lists available at ScienceDirect

Journal of Nuclear Materials

journal homepage: www.elsevier.com/locate/jnucmat

Compactibility and sintering behavior of nanocrystalline $(Th_{1-x}Ce_x)O_2$ powders synthesized by co-precipitation process

Ö. Yildiz [a,*], G. Modolo [b], R. Telle [c]

[a] Kocaeli University, Faculty of Engineering, Department of Metallurgical and Materials Engineering, TR-41380 Kocaeli, Turkey
[b] Institute for Energy Research and Reaktor Technology, Research Centre Jülich, D-52425 Jülich, Germany
[c] Institute of Mineral Engineering (Ceramic, Glass, Refractory and Building Materials) of RWTH Aachen, D-52064 Aachen, Germany

ARTICLE INFO

Article history:
Received 6 September 2007
Accepted 4 February 2008

ABSTRACT

Thoria (ThO_2) based ceramic material is a versatile and very important matrix for immobilization of plutonium and other tetravalent actinides either as a burning or a deposition material for final disposal. The aim of this study was to investigate the influence of the actinide concentration (simulated with cerium), the fabrication conditions and the properties of the produced powders on the compactibility and sinterability of the final products. The $(Th_{1-x}Ce_x)O_2$ powders with ceria concentration varying from 5 to 50 mol% were synthesized by co-precipitation method. The pellets were then compacted from calcined and ground powders at pressures varying from 250 to 750 MPa. The produced pellets had a homogenous grain size and sintered densities of 0.88% to 0.95% TD, respectively.

1. Introduction

The radioactive waste as decay products in nuclear reactors is separated according to its radioactive grade. The minor actinides (Pu, Np, etc.) should be deposited in a safe environment or further processed as a fuel after separation or extraction [1–7]. The thoria ceramic is a crucial material for immobilizing these tetravalent long-lived actinides, because of its face-centered cubic (fcc) fluorite-type crystal structure similar to these actinides dioxides [5,6,8–13]. The crystallized thoria is known to be a very insoluble material in aqueous media [9,10]. The thoria pellets with a high bulk-density are used as a blanket material in nuclear reactors [14,15].

The use of CeO_2 as a surrogate material instead of PuO_2 or of other tetravalent actinides is well-known. The ThO_2 and CeO_2 form almost an ideal solid solution in the complete composition range [4,16–20]. The dissolution behavior of CeO_2 and PuO_2 into a crystalline assembly and the overall shrinkage under the baseline sintering conditions is almost identical [19–21]. Therefore, the plutonium chemistry could be simulated using CeO_2 instead of highly active PuO_2. The CeO_2 and PuO_2 have quite similar physico-chemical properties, such as lattice constants, ionic sizes in octahedral and cubic coordination, melting points, standard enthalpy of formation, specific heat and thermal expansion behavior [4,12,17,19,22–25].

Barrier et al. fabricated $(Th_{1-x}Ce_x)O_2$ pellets from the powder containing 0–75% ceria synthesized by co-precipitation [26]. High pressures of 890 MPa were applied three times. The obtained densities of pellets reach values from 0.94 to 0.98 of theoretical density (TD), depending on the ceria content. It was observed that the addition of ceria (up to 20%) enhanced the sinterability of thoria [26]. Similar behavior was observed in the case of Pu [16,22,27].

Co-precipitation is a well-known fabrication method to synthesize mixed oxide ceramic powders such as ultra-fine nanocrystalline $(Th_{1-x}Ce_x)O_2$ powders at a relatively low calcination temperature [8,9,11,26,28,29]. The powder characteristics such as decomposition, crystallization, crystallite size, and specific surface area had been investigated depending on the ceria content (5–50 mol%), the calcination temperature, and the grinding solution [26,29]. Powders obtained by a co-precipitation process generally had a high surface area. This process is advantageous compared to the solid state synthesis of the bulk ceramic materials in terms of better compositional homogeneity and purity of the final product. The physical and chemical properties of nanocrystalline $(Th_{1-x}Ce_x)O_2$ powders depend upon the preparation conditions of the precursor and its thermal treatment [26,29]. Thus, the compactibility and sintering behavior of the powder should be a function of the powder characteristics and processing parameters. The knowledge of the interrelation between these parameters is particularly important in the fabrication of particles having reproducible properties.

In this work, the compactibility and sintering behavior of nanocrystalline $(Th_{1-x}Ce_x)O_2$ powders were studied to finally dispose of the minor actinides (Pu and the other with a +4 valence) as a stable solid solution in the ThO_2-based ceramic materials. The nanocrystalline $(Th_{1-x}Ce_x)O_2$ powders with varying ratios of ceria (5–50 mol%) were synthesized by co-precipitation process. The

* Corresponding author.
E-mail address: oyildiz@kou.edu.tr (Ö. Yildiz).

0022-3115/$ - see front matter © 2008 Elsevier B.V. All rights reserved.
doi:10.1016/j.jnucmat.2008.02.093

influence of the preparation conditions (the calcination temperature, the grinding solution of the powders, etc.) on the compactibility was investigated. The properties of the sintered product such as density, crystal structure and microstructure were determined.

2. Experimental procedures

2.1. Synthesis and characterization of $(Th_{1-x}Ce_x)O_2$ powders

The $(Th_{1-x}Ce_x)(OH)_4$ powders were prepared using $Th(NO_3)_4 \cdot 5H_2O$ (Merck, 99 wt% purity) and $Ce(NO_3)_3 \cdot 6H_2O$ (Alfa Aesar, 99.5 wt% purity) as starting materials. Ammonia gas (99.98%) and distilled water were used as precipitator and solvent, respectively. The details of the preparation of $(Th_{1-x}Ce_x)O_2$ powders were published in a recent work [29]. The precipitates were dried in air at 110 °C and then calcined at different temperatures (300, 420 and 600 °C) before and/or after wet grinding of the agglomerate powders in different solvents with ball milling. The influence of the two steps calcination process on the powder properties and densification behavior was studied by recalcining one of the 300 °C calcined powder at 600 °C after grinding once more. The grinding of one of the sample was performed in different solvents (acetone, carbon tetrachloride (CCl_4), isopropanol and water) to compare the influence of the grinding solution on the specific surface area and compactibility.

Previously [29], the characterization of the $(Th_{1-x}Ce_x)(OH)_4$ powders was carried out by using several techniques such as the differential thermal analysis (DTA) with thermogravimetric analysis (TGA), X-ray powder diffraction (XRD), transmission electron microscope (TEM) and BET method to investigate the thermal behavior and physical properties such as phase transformation, crystallization, crystal structure, solid solution formation, morphology, grain size and specific surface area of powders.

2.2. Fabrication and characterization of green and sintered pellets

The powders, which were calcined at various temperatures and ground in different solvents, were compacted in the form of cylindrical pellets of 10 mm diameter using a uniaxial hydraulic press with pressing pressures between 250 and 750 MPa. The green density (GD) of the compacts was determined by weighing and geometrical calculation. The green pellets were sintered at 1500 °C for 5 h in air atmosphere using a Linn HT 1800 electric resistance furnace (Linn Electronic Co., Germany). The heating rate was 5 °K/min.

The microstructures of the sintered pellets were investigated by scanning electron microscopy (SEM) using JEOL JSM840. The samples were prepared by metallographic techniques and then thermally etched in air at 1450 °C for 1 h. The crystal structure and the unit cell parameters of the sintered pellets were investigated by XRD analysis by STOE & Cie STADI P Diffractometer using Co Kα radiation with a characteristic wavelength $\lambda = 0.178897$ nm $2\theta = 5–85°$) at room temperature. The theoretical densities (TD) of the sintered $(Th_{1-x}Ce_x)O_2$ pellets were calculated from the XRD data. The densities of the sintered pellets were determined by the Archimedes principle.

3. Results and discussion

3.1. Compactibility of $(Th_{1-x}Ce_x)(OH)_4$ powders

The particle size distribution of $(Th_{0.9}Ce_{0.1})(OH)_4$ powder containing 10% of ceria, which was calcined at 420 °C, was investigated before and after grinding using an optical microscope with a computer connection (Fig. 1). The particle size distribution ranged between 5–300 μm before grinding and about 120 μm (maximum at 30 μm) after grinding. The particle sizes less than 1 μm could not been determined since these aggregates were transparent. Before grinding, ca. 40% of powder particles were below 10 μm and after grinding the powder had a particle size distribution below 10 μm (ca. 95%). The specific surface area of $(Th_{1-x}Ce_x)(OH)_4$ powders increased by heat treatment up to ca. 420 °C and decreased above 600 °C due to sintering effect of the heat treatment on the powders. The TEM micrograph shows the morphology of the $(Th_{0.95}Ce_{0.05})(OH)_4$ powders which were heated at 800 °C after grinding (Fig. 2). One of the possible reasons for agglomeration could be the diffusion of fine particles (nanoparticles) starting at low temperatures. A broader particle size distribution was obtained for the samples which were calcined between 300 and 600 °C, while the powders calcined higher than 600 °C had the largest particle size distribution range.

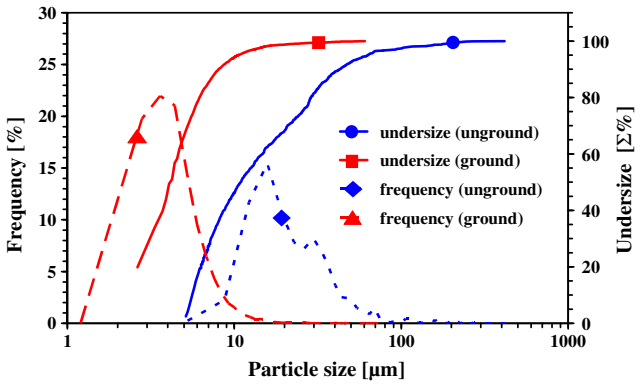

Fig. 1. Influence of grinding on aggregate size of $(Th_{0.9}Ce_{0.1})(OH)_4$.

The effect of calcination temperature on the green density with various pressing pressures was shown in Fig. 3. In all cases, a linear relationship between green density and compaction pressure was observed. An increase in temperature (until 600 °C) also increased the green density. The compacted pellets produced from these powders had a very high relative green density although the powders calcined at 600 °C had a less specific surface area as they contain large particles in a considerable percentage [29]. In this work, it was recognized that the particle size distribution had a very important influence on the compactibility of powders. An increase in the calcination temperature had a positive influence on the green density up to 600 °C (Fig. 3). Very fine particle size (high specific surface area) and a wide particle size distribution were obtained as the powders were calcined at less than 420 °C before

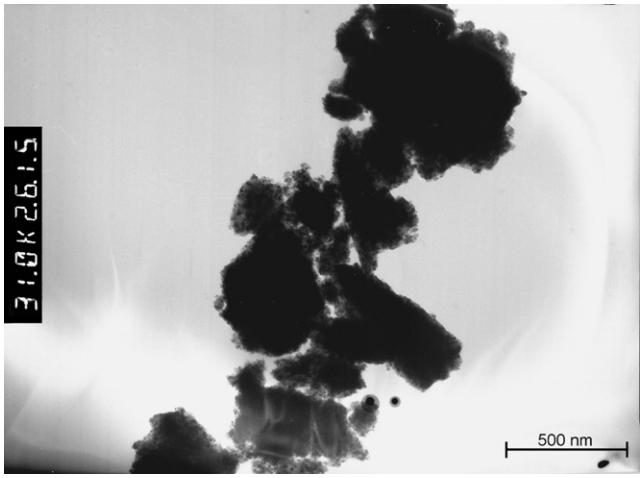

Fig. 2. TEM image of $(Th_{0.95}Ce_{0.05})(OH)_4$ agglomerate sintered at 800 °C.

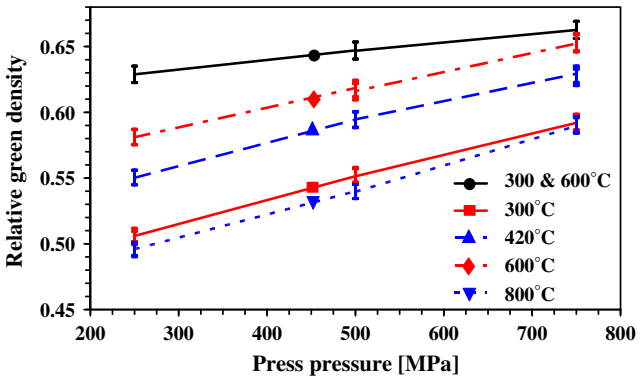

Fig. 3. The effect of calcining temperature on the green density of compacted pellets from $(Th_{0.75}Ce_{0.25})(OH)_4$ powders.

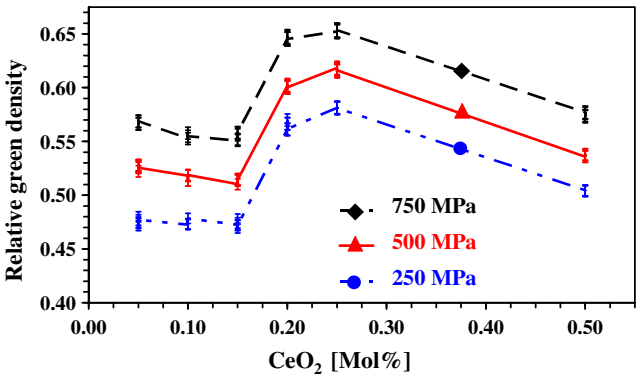

Fig. 5. The effect of CeO_2 content on the green density of compacts (powders calcined at 600 °C and ground in acetone).

grinding and at 600 °C after grinding. The highest relative green density was obtained from the powders, which were calcined at 300 °C before grinding and 600 °C after grinding (66% of TD). The particle size largely depends on the firing temperature. The heat treatment above 600 °C had a sintering effect on the powders. Therefore, when the powders were calcined at high temperatures greater than 600 °C, the grinding of these powders becomes difficult due to coarsening and formation of hard sinter agglomerates. Thus the compacts from these powders had the lowest green density (Fig. 3, see 800 °C).

The influence of grinding media on the green density of compacted pellets as a function of compaction pressure ($250 \leqslant P \leqslant 750$ MPa) was investigated (Fig. 4). The grinding solutions acetone and CCl_4 had similar effects on the green density. These pellets had a green density greater than 0.6% of TD. The pellets obtained from powders, which were ground in isopropanol and water, had lower green densities (Fig. 4), because the surface tension of the grinding media affects the wettability and grinding performance of the powders. Another influence on the compaction density comes from the polarity of the dispersion medium which is increasing in the order CCl_4 < acetone < isopropanol < water. If the dipole moment of the dispersion molecules is large, a well-oriented interconnection of the oxide powder surfaces occurs resulting in stronger Van-der-Waals bonding between the particles after drying. This in turn, yields aggregates which are difficult to deform during pressing.

The influence of the ceria concentration on the compactibility is shown in Fig. 5. The initial decrease observed in the graph is an expected effect of the decrease in the BET specific surface area. The graph shows an increase in the green density for the powders containing more than 0.15 mol% CeO_2 despite the fact that powders having lower specific surface areas yielding lower green densities. The reason of this behavior could be attributed to the role of ceria on the morphology and particle size distribution of the powder. Above 0.25 mol% CeO_2 the decrease in the specific surface area would no longer be compensated by morphology and particle size effects and the density again falls off. It was clearly seen, that powder processing steps such as precipitation, drying, calcining and grinding conditions had very important results on the powder characteristics and compactibility because these affect the particle size distribution, agglomerate shape, and hardness of the powders. Three level processing steps such as calcining, grinding and re-calcination process resulted in higher compactibility. In three steps, the powders were calcined at low temperature (300 °C) and then ground in acetone and the ground powders were recalcined again at higher temperature at 600–800 °C. The best powder compactibility was obtained by this process (Fig. 3). The determination of the optimum calcining temperature before grinding is very important. In general, a linear relation between green density, calcining temperature and pressing pressure were observed, but cracks in green pellets were formed after ca. 900 MPa.

3.2. Sintering behavior of $(Th_{1-x}Ce_x)(OH)_4$ pellets

The sinterability of the compacts obtained between 250 MPa and 750 MPa was investigated according to different preparation conditions of the starting powders $(Th_{1-x}Ce_x)(OH)_4$ [calcinations at different temperatures between 300 and 800 °C and grinding in different solutions (acetone, CCl_4, isopropanol and water)].

The green density of the compacts showed a clear trend as a function of the calcination temperature, but the influence of calcination temperature on the sintered density was not the same (Figs. 3 and 6). Although the compacts from the powder calcined at 600 °C had a larger green density in the range (58–65% of TD) than the compacts from powder calcined at 300 °C (50–59% of TD)

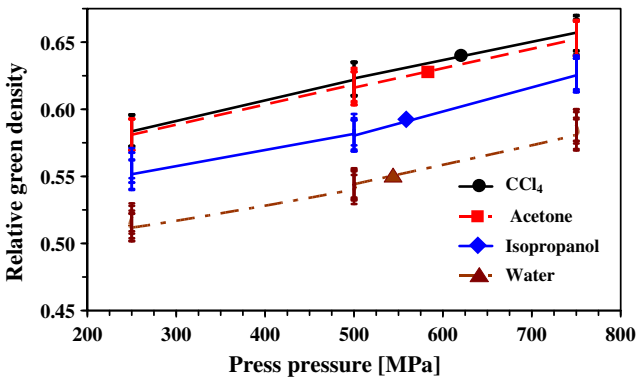

Fig. 4. Effect of grinding solution on the green density of the $(Th_{0.75}Ce_{0.25})(OH)_4$ compacts (powders calcined at 600 °C).

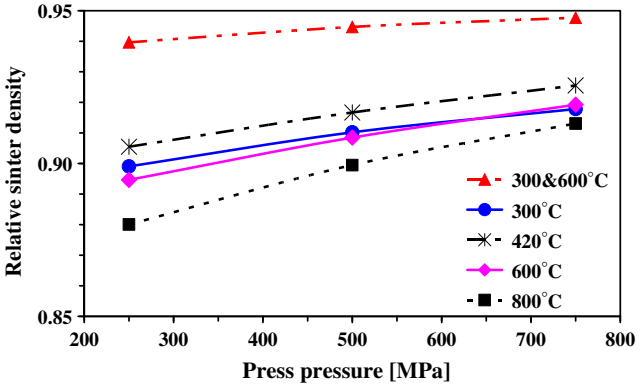

Fig. 6. The influence of calcining temperature on the relative sinter density of the pellets from the $(Th_{0.75}Ce_{0.25})(OH)_4$ powders ground in acetone.

(Fig. 3). The sintered density of the compacts ranged between 89–91% and 90–92% of TD, respectively (Fig. 6). The calcination temperature up to 600 °C had a positive influence on the green density (Fig. 3) but it did not show the same correlation for the sintered density (Fig. 6). In addition, the great density differences in green pellets were much more smaller in the sintered samples. The highest sintered density (similar for the green density) was obtained from the powders, which were calcined at 300 °C before grinding and recalcined at 600 °C (95% of TD).

Fig. 7 shows the sintered density of the pellets obtained from $(Th_{0.75}Ce_{0.25})(OH)_4$ powders calcined at 420 °C and then ground in acetone, CCl_4, isopropanol and water. The results show that acetone and CCl_4 had the same effect on the specific surface area [29] and green density as in Fig. 4, but the powders ground in acetone had much better sinterability with greater than 90% TD (Fig. 7). Here, it was observed that the use of acetone as a milling media causes a well dispersed powders due to improved wetting which in turn results in a better sintering behavior during the densification process. If a high sinter density of the end product is not important or desired, water could be chosen as a milling media. Acetone was preferred as a milling media in this work because of its high performance. The recovery of acetone from process was also very easy and economic. But, it should not be forgotten that acetone is flammable and more expensive than water.

The ceria addition in ThO_2 decreased clearly the specific surface area of the $(Th_{1-x}Ce_x)O_2$ powder [29], but it increased the sinterability of the powder until 25 mol% ceria (Fig. 8). The $(Th_{0.75}Ce_{0.25})(OH)_4$ powder had a specific surface area lower than $(Th_{0.95}Ce_{0.05})(OH)_4$ [29], but the sintered density of $(Th_{0.75}Ce_{0.25})O_2$ pellets was higher than $(Th_{0.95}Ce_{0.05})O_2$ (Fig. 8).

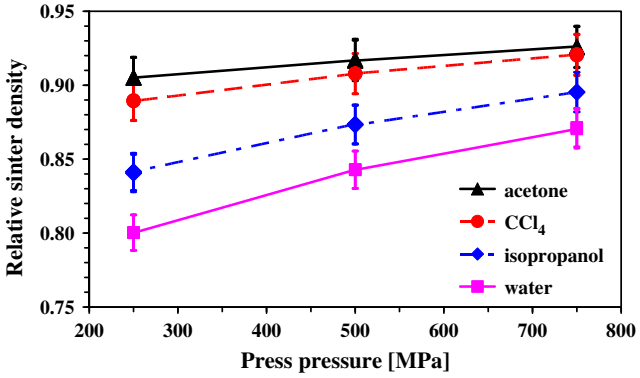

Fig. 7. Influence of grinding solution on the relative sinter density of the pellets from the $(Th_{0.75}Ce_{0.25})(OH)_4$ powders calcined at 420 °C.

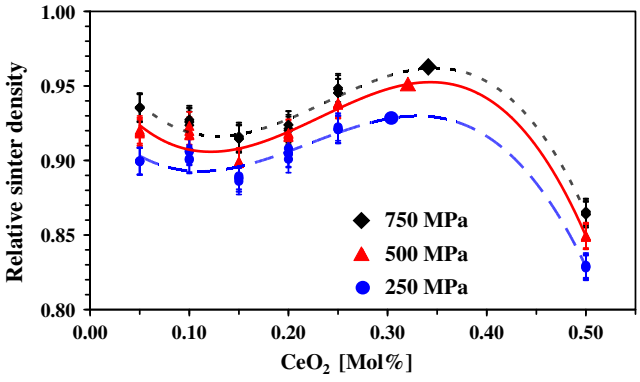

Fig. 8. Influence of CeO_2 content on the relative sinter density of the compacts (powders calcined at 600 °C and ground in acetone).

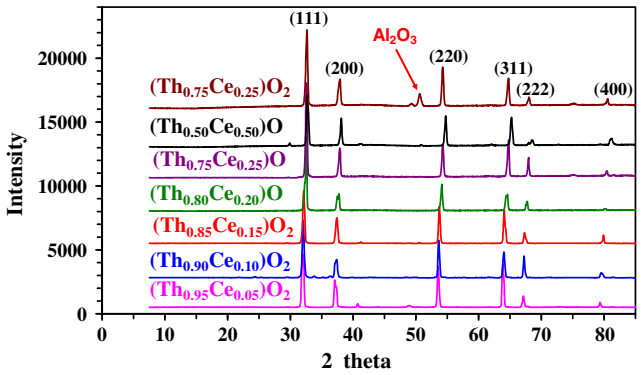

Fig. 9. XRD patterns of the $(Th_{1-x}Ce_x)O_2$ pellets sintered at 1500 °C for 5 h in air. Al_2O_3 from grinding ball.

The results showed that the ceria concentration up to 25 mol% had a positive influence on the sinterability, although the specific surface area decreases. But after this point, the increase in the amount of ceria was not sufficient to compensate the decrease in the specific surface area causing the density to decrease. Barrier et al. observed that the addition of ceria (up to 20%) to the $(Th_{1-x}Ce_x)O_2$ pellets enhanced the sinterability of thoria [26]. A similar behavior was also observed in the case of Pu [16,22,27]. Therefore, the specific surface area (the average particle size interrelation) should not be used as a single parameter to argue sinter activity. A direct correlation of sinterability with specific surface area or with ceria concentration is not decisive since both factors affect the sinterability contrary to each other (Fig. 8). The influence of ceria was also seen in X-ray diffraction. The samples with higher ceria content crystallized at a lower temperature and these had a stronger intensity in the XRD peaks than those of the other samples with less ceria additions [29]. The same results were obtained in the end products as well (Fig. 9).

The crystal structure of sintered pellets with various ceria contents were examined by XRD, as shown in Fig. 9. The pellets were sintered at 1500 °C for 5 h in air. It is well-known that there are several parameters (particle size, ceria contents etc.) which affect the X-ray diffraction lines. The XRD analyses showed that all products form a solid solution according to the starting compositions (Fig. 9). Al_2O_3 peaks were determined in some of the samples (Fig. 9, uppermost) probably contamination coming from the

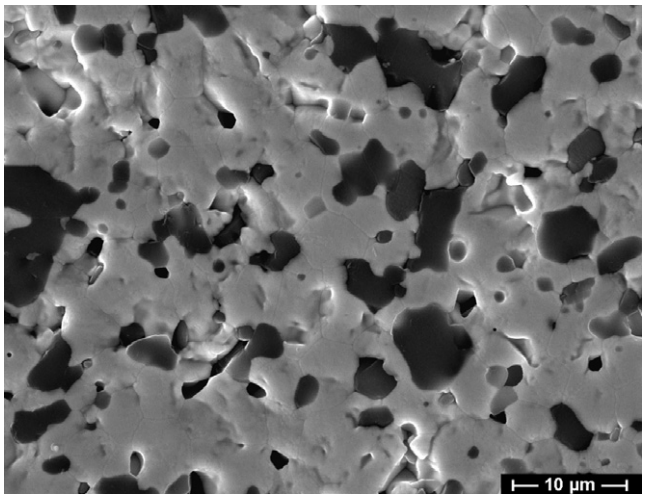

Fig. 10. Microstructure of Al_2O_3-containing sample. Powders calcined at 800 °C and ground in acetone. Pellets sintered at 1500 °C for 5 h in air.

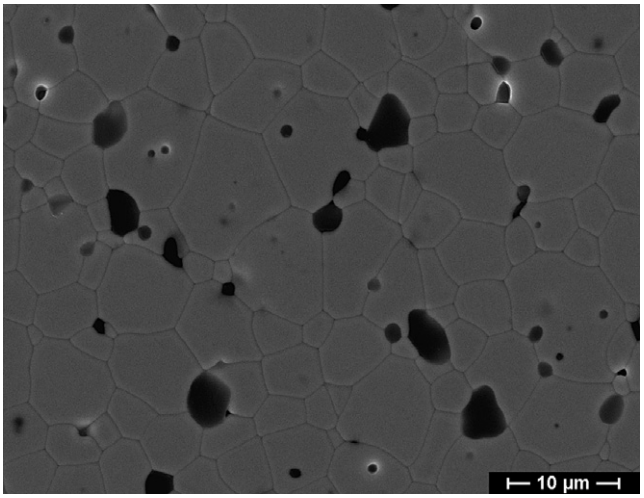

Fig. 11. Microstructure of the $(Th_{0.75}Ce_{0.25})O_2$ pellet prepared from the powders calcined at 300 °C, ground in acetone, recalcined at 600 °C, sintered at 1500 °C for 5 h in air.

Al_2O_3 milling balls. The quality of the grinding balls was not very good and the grinding time for the powder calcined at higher temperature was very long (6 h). The heat treatment above 600 °C had a sintering effect on the powders and thus the powders coarsened and formed hard agglomerates. Therefore the impurities come from the grinding ball (Fig. 10). The microstructure of the $(Th_{0.75}Ce_{0.25})O_2$ pellet, which was prepared from the powder calcined at 300 °C before grinding in acetone and at 600 °C after grinding and sintered at 1500 °C for 5 h, showed that the grains were small and almost uniform (Fig. 11). This sample had a relative sintered density of 95% TD (cf. Fig. 6). Most of the black areas in Figs. 10 and 11 are the impurity from grinding mill.

It is also well-known that the above mentioned properties such as very small particle size (high specific surface area), very wide particle size distribution, quantity of the spherical particles (morphology) and hardness of the agglomerate (dependent on the calcination temperature) had an influence on the sinterability of the ceramic materials. The starting powders, $(Th_{1-x}Ce_x)(OH)_4$, had very small particle (crystallite) sizes, high surface areas and spherical particle form [29]. Although the changes in properties of the powders correlated generally with the change in sintered density, the parameters were not directly resembled in the sintering behavior in total.

In a previous work the powder properties such as reactivity, morphology, surface texture, particles size and shape was studied [29]. These properties affect the compactibility and sintering behavior of the powders which was further investigated in this study. It was observed that the ceria concentration in starting materials had a positive influence on the sinterability of thoria ceramics. The highest density (95% of TD) was obtained from the powder which contained 25 mol% ceria, which was calcined at 300 °C before grinding and recalcined at 600 °C after grinding in acetone and was pressed with 750 MPa (Figs. 6 and 11). As indicated in the introduction the aim of this study was not to produce only dense pellets. The products could be modified according to its application and be used for different purposes.

4. Conclusions

The knowledge of the quantitative sintering kinetics of the $(Th_{1-x}Ce_x)O_2$ powders is very important for the ceramic industry and especially for the nuclear fuel manufacturers. The thermal behavior, degree of crystallization specific surface area, and average crystallite size of $(Th_{1-x}Ce_x)O_2$ powders were studied in a former work while the influence of these properties on the compactibility and sintering behaviors were presented here. Nanocrystalline $(Th_{1-x}Ce_x)O_2$ powders could easily be synthesized using co-precipitation process. When the powders were first ground after calcining at 300 °C (or <300 °C) and then recalcined at 600 °C (max. 800 °C), they have excellent compactibility and sintering behavior. The determination of the suitable calcination temperature before and after grinding is very crucial. The experimental works showed that any changes in the preparation parameters of powders such as the heat treatment temperature and grinding conditions had a great influence on the powder characteristics. For example: small differences in the preparation conditions change directly the aggregate morphology (the agglomerate hardness, form and size), specific surface area, and activity of powders. These influenced the powder behavior, e.g. compactibility and sinterability.

Acknowledgements

This work had been carried out within the frame of a research program of Helmholtz Association of National Research Centres (HGF) (at Institute for Safety Research and Reactor Technology (ISR) in Research Centre (FZ) Jülich). The authors would like to thank Professor Dr R. Odoj at ISR in FZ Jülich for their support, and advice. We also thank to Dr A. Bukaemskiy, Dipl.- Ing. H. Vijgen, Dr M. Titov at ISR and W. Reichert at ZCH for their friendly help.

References

[1] M. Mariani, E. Macerata, M. Galletta, A. Buttafava, A. Casnati, R. Ungaro, A. Faucitano, M. Giola, Radiat. Phys. Chem. 76 (2007) 1285.
[2] P. Taylor, W.H. Hocking, T. Lawrence, H. Johnson, R.J. Mceachern, S. Sunder, Nucl. Technol. 116 (1996) 222.
[3] N. Dacheux, R. Podor, B. Chassigneux, V. Brandel, M. Genet, J. Alloy Compd. 271 (1998) 236.
[4] K. Bakker, E.H.P. Cordfunke, R.J.M. Konings, R.P.C. Schram, J. Nucl. Mater. 250 (1997) 1.
[5] W. Lutze, R.C. Ewing, Radioactive Waste Forms for the Future, 8, Elsevier, Amsterdam, 1988, p. 495.
[6] W.L. Gong, W. Lutze, R.C. Ewing, J. Nucl. Mater. 277 (2000) 239.
[7] Thorium as a waste management option, Final Report of European Contract, No. FI4I/CT95011, 1999.
[8] S. Hubert, J. Purans, G. Heisbourg, P. Moisy, N. Dacheux, Inorg. Chem. 45 (2006) 3887.
[9] S. Hubert, K. Barthelet, B. Fourest, G. Lagarde, N. Dacheux, N. Baglan, J. Nucl. Mater. 297 (2001) 206.
[10] C.F. Baes, R.E. Mesmer, The Hydrolysis of Cations, Wiley-Interscience, New York, 1976. p. 129.
[11] S. Hubert, G. Heisbourg, N. Dacheux, J. Ritt, 7th IMF, Petten 2526, October, 2001.
[12] A.K. Tyagi, B.R. Ambekar, M.D. Mathews, J. Alloy Compd. 337 (2002) 277.
[13] Gmelin Handbuch, Thorium, SystemNr 44, Ergänzungsband Teil C2, 1976, p. 78.
[14] R.D. Purohit, S. Saha, A.K. Tyagi, J. Nucl. Mater. 288 (2001) 7.
[15] V. Chandramouli, S. Anthonysamy, P.R. Vasudeva Rao, J. Nucl. Mater. 265 (1999) 255.
[16] M.D. Freshley, H.M. Mattys, General Electric Report HW-76559, 1962, p.116, US Atomic Energy Commission Report, Oak Ridge, Tenn., February 1968, p. 463.
[17] M.D. Mathews, B.R. Ambekar, A.K. Tyagi, J. Nucl. Mater. 288 (2001) 83.
[18] M.D. Mathews, B.R. Ambekar, A.K. Tyagi, J. Nucl. Mater. 280 (2000) 246.
[19] J.C. Marra, A.D. Cozzi, R.A. Pierce, J.M. Pareizs, A.R. Jurgensen, D.M. Missimer, Cerium as a Surrogate in the Plutonium Immobilized Form, in WSRCMS200100007, Contract No. DEAC0996SR18500.
[20] Y.W. Lee, H.S. Kim, S.H. Kim, C.Y. Young, S.H. Na, G. Ledergerber, P. Heimgarbner, M. Pouchon, M. Burghartz, J. Nucl. Mater. 274 (1999) 7.
[21] C. Ganguly, in: I.J. Hasting (Ed.), Second International Conference on CANDU Fuel, Pembroke, Ontario, Canada, 1989, p. 398.
[22] T.R.G. Kutty, K.B. Khan, P.V. Hegde, A.K. Sengupta, S. Majumdar, D.S.C. Purushotham, J. Nucl. Mater. 297 (2001) 120.
[23] M.D. Freshley, H.M. Mattys, General Electric Report HW76559, 1962, p. 11.6.
[24] J.G. Pepin, G.J. McCarthy, J. Am. Ceram. Soc. 64 (9) (1981) 511.
[25] A.K. Tyagi, M.D. Mathews, J. Nucl. Mater. 278 (2000) 123.
[26] D. Barrier, A.A. Bukaemskiy, G. Modolo, J. Nucl. Mater. 352 (2006) 357.
[27] T.R.G. Kutty, P.V. Hegde, J. Banerjee, K.B. Khan, A.K. Sengupta, G.C. Jain, S. Majumdar, H.S. Kamath, J. Nucl. Mater. 312 (2003) 224.
[28] B.C. Sales, C.W. White, L.A. Boatner, Nucl. Chem. Waste Manage. 4 (1983) 281.
[29] Ö. Yildiz, J. Nucl. Mater. 366 (2007) 266.